Effects of Properties and Simulations for Dry Granular Soils on Buckling Loads of Portal Frames

Dr. Salah R. Al Zaidee
Lecturer, Civil Eng. Dept.
College of Engineering, University of Baghdad
Teghreed H. Ibrahim
Assistance lecturer, Civil Eng. Dept.
College of Engineering, University of Baghdad
Ehab G. Al Hasany
M. Sc. Student, Civil Eng. Dept.,
College of Engineering, University of Baghdad

Abstract:-

This paper aims to use different finite element models to show how different soil conditions and different soil simulations can affect buckling loads for portal frames. All soils are assumed granular and dry while spread footing is assumed for foundation system.
Two soil simulations have been adopted. In the first simulation, Winkler's foundations is used where continuous soil media has been replaced with uncoupled springs. Shear forces between adjacent soil prisms and the corresponding stiffness are both lost in this simulation. In the second model, soil mass under footing have been isolated and simulated with brick elements.
Soil elastic modulus and Poisson ratio have been estimated based on correlations with the SPT value.
Results indicate that, the critical loads determined with hinge simulation of spread footing are underestimated compared with the more accurate value of soil mass simulation, while critical loads estimated from fixed supports simulation are close to that of soil mass simulation even for compressible soils with SPT value in the range of 10.
Critical loads determined from Winkler soil simulation are close to those loads of soil mass simulation with a difference not greater than 7% and with correlation coefficient of 0.99. Two logarithmic functions, have been developed based on nonlinear regression analyses.

Keywords: - Buckling loads, portal steel frame, finite element analysis, Winkler's model, simulation of soil mass.

I. Introduction

It is well known, theoretically and experimentally, that different support conditions have significant effects on buckling strength of steel structures.
To simplify analysis process, ideal supports including fixed, hinge, and roller are usually used in engineering practice to simulate actual foundation systems that physically located in a transition zone between the extreme ideal conditions. Portal frames similar to that presented in **Fig. 1** is usually adopted in single story buildings for industrial, warehousing or other purposes.

Depending on span and soil conditions, spread footings with/without tie beams or continuous footings may be used to support such a portal frame. In design practice, these footings may be simulated as hinges when they are relatively flexible and soil is compressible or simulated as fixed when they are relatively stiff and soil is incompressible. Between these two modeling extremes, there is a vast transition zone where soil-structure interaction has an impact on behavior of the frame and foundation.

In this paper, the finite element method is used to show how soil structure interaction can affect buckling loads for portal frames supported on spread footings. Different dry granular soils starting from compressible soil with SPT value of 10 to stiff soil with SPT value of 50 have been considered.

Two models have been adopted to simulate soil stiffness. In the first one, Winkler model with uncoupled linear springs has been adopted. While three-dimensional solid element has been adopted in the second simulation.

II. Finite Element Model

A. Overview

Due to existing of purlins and bracings indicated in **Fig. 1** below, designers usually concern with sway and non-sway buckling modes that produce bending moments about major axes of rafters and columns [1].

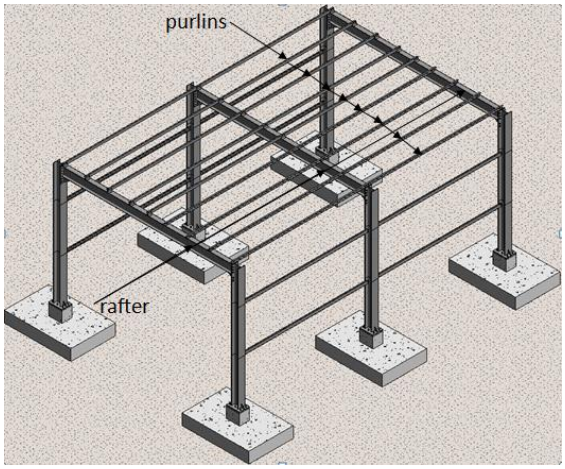

Fig. 1 Portal frame.

To reflect this fact, a typical interior frame indicate in **Fig. 2** below has been considered with indicated symmetry plane to enforce the frame to buckle in the plane where sway and non-sway modes produce bending moments about major axes only.

B. Modeling of Rafter, Columns, and Pedestals

Space frame element with six d.o.f., three translational and three rotational, indicated in **Fig. 3** below is used to simulate steel rafters, columns, and concrete pedestals.

According to reference [2], this element has an explicit stiffness matrix indicated in **Fig. 4** below.

When interaction between axial force and bending moment is included for a space frame element, member stiffness matrix is reduced by geometric stiffness matrix indicated in **Fig. 5** below, [3].

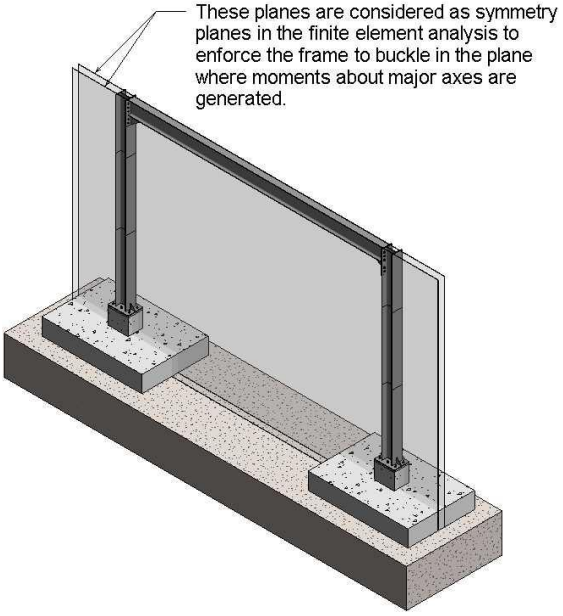

Fig. 2 A typical internal frame that considered in finite element simulation of this study.

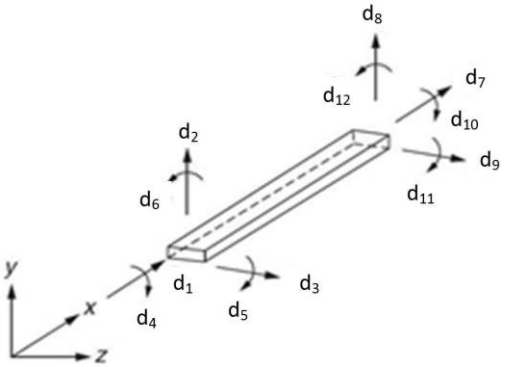

Fig. 3 Space frame element with 6 dof per node adopted in simulate of purlins, rafters, and columns.

$$[k^{(e)}]_{12\times 12} = \begin{bmatrix} \frac{EA}{l} & & & & & & & & & & & \\ 0 & \frac{12EI_{zz}}{l^3} & & & & & & & & & & \\ 0 & 0 & \frac{12EI_{yy}}{l^3} & & & & & & & & & \\ 0 & 0 & 0 & \frac{GJ}{l} & & & & & & & & \\ 0 & 0 & \frac{6EI_{yy}}{l^2} & 0 & \frac{4EI_{yy}}{l} & & & & & & & \\ 0 & \frac{6EI_{zz}}{l^2} & 0 & 0 & 0 & \frac{4EI_{zz}}{l} & & & & & & \\ -\frac{EA}{l} & 0 & 0 & 0 & 0 & 0 & \frac{EA}{l} & & & & & \\ 0 & -\frac{12EI_{zz}}{l^3} & 0 & 0 & 0 & -\frac{6EI_{zz}}{l^2} & 0 & \frac{12EI_{zz}}{l^3} & & & & \\ 0 & 0 & -\frac{12EI_{yy}}{l^3} & 0 & -\frac{6EI_{yy}}{l^2} & 0 & 0 & 0 & \frac{12EI_{yy}}{l^3} & & & \\ 0 & 0 & 0 & -\frac{GJ}{l} & 0 & 0 & 0 & 0 & 0 & \frac{GJ}{l} & & \\ 0 & 0 & \frac{6EI_{yy}}{l^2} & 0 & \frac{2EI_{yy}}{l} & 0 & 0 & 0 & -\frac{6EI_{yy}}{l^2} & 0 & \frac{4EI_{yy}}{l} & \\ 0 & \frac{6EI_{zz}}{l^2} & 0 & 0 & 0 & \frac{2EI_{zz}}{l} & 0 & -\frac{6EI_{zz}}{l^2} & 0 & 0 & 0 & \frac{4EI_{zz}}{l} \end{bmatrix} \begin{matrix} d_1 \\ d_2 \\ d_3 \\ d_4 \\ d_5 \\ d_6 \\ d_7 \\ d_8 \\ d_9 \\ d_{10} \\ d_{11} \\ d_{12} \end{matrix}$$

Symmetric

Fig. 4 Explicit stiffness matrix for space frame element.

$$[k_g^{(e)}]_{12\times 12} = \frac{P_x}{L} \begin{bmatrix} 1 & 0 & 0 & 0 & 0 & 0 & -1 & 0 & 0 & 0 & 0 & 0 \\ & \frac{6}{5} & 0 & 0 & 0 & \frac{L}{10} & 0 & -\frac{6}{5} & 0 & 0 & 0 & \frac{L}{10} \\ & & \frac{6}{5} & 0 & -\frac{L}{10} & 0 & 0 & 0 & -\frac{6}{5} & 0 & -\frac{L}{10} & 0 \\ & & & \frac{J}{A} & 0 & 0 & 0 & 0 & 0 & -\frac{J}{A} & 0 & 0 \\ & & & & \frac{2L^2}{15} & 0 & 0 & 0 & \frac{L}{10} & 0 & -\frac{L^2}{30} & 0 \\ & & & & & \frac{2L^2}{15} & 0 & -\frac{L}{10} & 0 & 0 & 0 & -\frac{L^2}{30} \\ & & & & & & 1 & 0 & 0 & 0 & 0 & 0 \\ & & & & & & & \frac{6}{5} & 0 & 0 & 0 & -\frac{L}{10} \\ & & & & & & & & \frac{6}{5} & 0 & \frac{L}{10} & 0 \\ & & & & & & & & & \frac{J}{A} & 0 & 0 \\ & & & & & & & & & & \frac{2L^2}{15} & 0 \\ & & & & & & & & & & & \frac{2L^2}{15} \end{bmatrix} \begin{matrix} d_1 \\ d_2 \\ d_3 \\ d_4 \\ d_5 \\ d_6 \\ d_7 \\ d_8 \\ d_9 \\ d_{10} \\ d_{11} \\ d_{12} \end{matrix}$$

Sym

Fig. 5 Geometric stiffness for space frame element, adopted from reference[3].

C. Connections between Members

Fully rigid connections have been adopted to simulate girder to column connection, and column to pedestal connection indicted in **Fig. 6** below. With this connections type the frame can withstand loads without bracing.

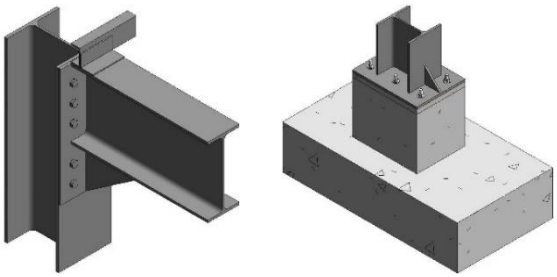

(a) (b)

Fig. 6 Rigid connection, (a) Girder to column, (b) Column to pedestal.

C. Modeling of Spread Footing

Quadrilateral shell element with a typical node indicated in **Fig. 7** is adopted to simulate spread footings. There is no substantial membrane forces in foundation, but it has been included, i.e. shell element instead of plate element is adopted, to generalize the model and to make assemblage process more straightly.

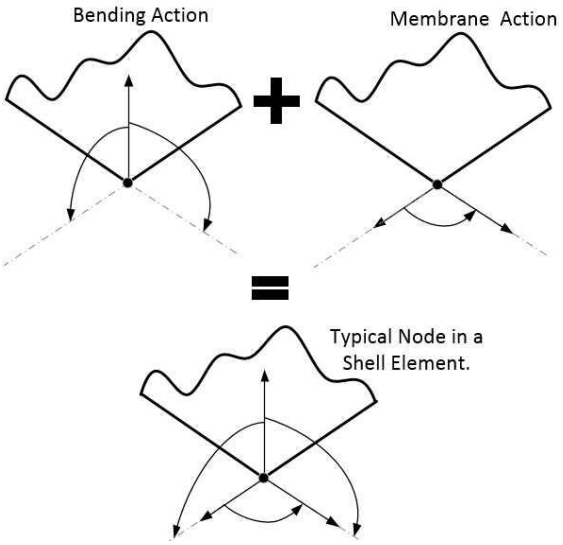

Fig. 7 Typical node for quadrilateral shell element adopted to simulate foundations.

D. Soil Modeling

1) Winkler Model

In the Winkler simulation, the soil continuum is replaced by uncoupled springs with stiffness,k_s, usually called a coefficient of subgrade reaction, as shown in **Fig. 8**.

Springs underneath each element are lumped to element nodes according to displacement field that already adopted in the formulation of the shell element, a *consistence formulation*.

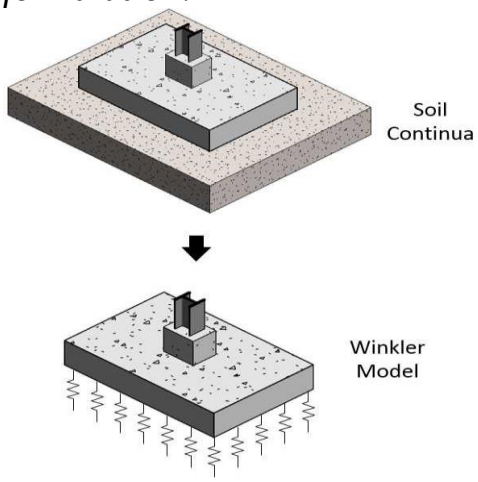

Fig. 8. Winkler model for soil continuum.

2) Soil Mass Model

In the second soil simulation, a soil mass located under spread footing has been isolated and simulated using trilinear (eight-node) hexahedron with geometry and d.o.f. as illustrated in **Fig. 9** below. With many element along soil depth, as shown in **Fig. 10**, even possible bending model can be simulated with this element [4].

Based on analytical solutions of theory of elasticity, planes where soil mass has been isolated from its semi-infinite media have been located such that stresses and strains in soil mass are almost fully dissipated [5].

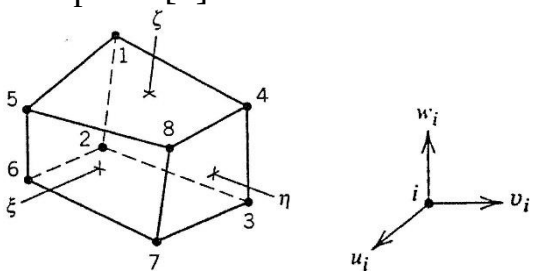

(a) (b)

Fig. 9 Trilinear hexahedron, geometry and typical d.o.f.

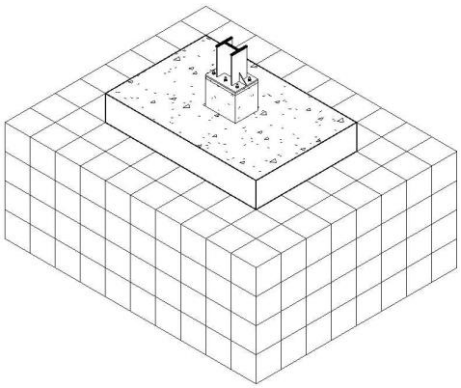

Fig. 10. Finite element model and mesh for soil mass.

E. Material Properties

Steel for rafter and columns and concrete for pedestals and spread footing are assumed linear and elastic.

Dry granular soils adopted in this study have been defined in terms the SPT value. All other soil properties pertained to the finite element models of this study have been determined based on appropriate correlations with the SPT value.

According to reference [6], coefficient of subgrade reaction, k_s, can be related to soil allowable bearing capacity, $q_{allowable}$, based on equation(***(1***).

$$k_s = 40\ q_{ultimate} \qquad (1)$$

According to reference [7] the relation indicated in equation (2) below can be used to correlate the angle of internal friction, ϕ, to SPT value.

$$\phi = 27.1 + 0.3N - 0.00054(N)^2 \qquad (2)$$

In turn, the angle of internal friction, ϕ, can be related to soil bearing capacity based on traditional equations of bearing capacity. Adopting Meyerhof equation with dropping of cohesion and surcharge terms, relation between ϕ and $q_{ultimate}$ reduce to that indicated in equation (***(***3) below.

$$q_{ultimate} = 0.4\gamma B N_\gamma s_\gamma \qquad (3)$$

where the parameter N_γ is determined based on the following relation:

$$N_\gamma = (N_q - 1)\tan(1.4\phi)$$

$$N_q = e^{\pi tan\phi} \tan^2\left(45 + \frac{\phi}{2}\right)$$

The shape factor, s_γ, is determined as follows:

$$s_\gamma = 1 + 0.1 \tan^2\left(45 + \frac{\phi}{2}\right)\frac{B}{L}$$

According to reference [8], the elastic modulus, E_s, of granular soils can be related to standard penetration number, N, based on equation ***(*** *4*) below:

$$E_s = 10 p_a N \qquad (4)$$

Where p_a is the atmospheric pressure, approximately equal to $100\ kPa$.

meanwhile Poisson ratio for cohesionless soils, ν_s, can be related to its angle of internal friction, ϕ, based on equation (***(*** 5) below[8].

$$\nu_s = 0.1 + 0.3\left(\frac{\phi - 25}{20}\right) \qquad (5)$$

F. Mesh Size

As indicated in **Fig. 11**, in traditional stiffness or displacement analysis, loads between member ends are simulated as a fixed end forces with un-balanced forces acting on nodes only[9].

For frame members subjected to nodal forces only, cubical displacement represents an exact solution and whole member length can be simulated with a single element. At buckling critical state, columns has trigonometric deflected shape and their lengths should be discretized into a relatively fine mesh of the element based on cubical displacement shape. Therefore, a mesh size of 0.1m has been adopted for the beam and the two columns.

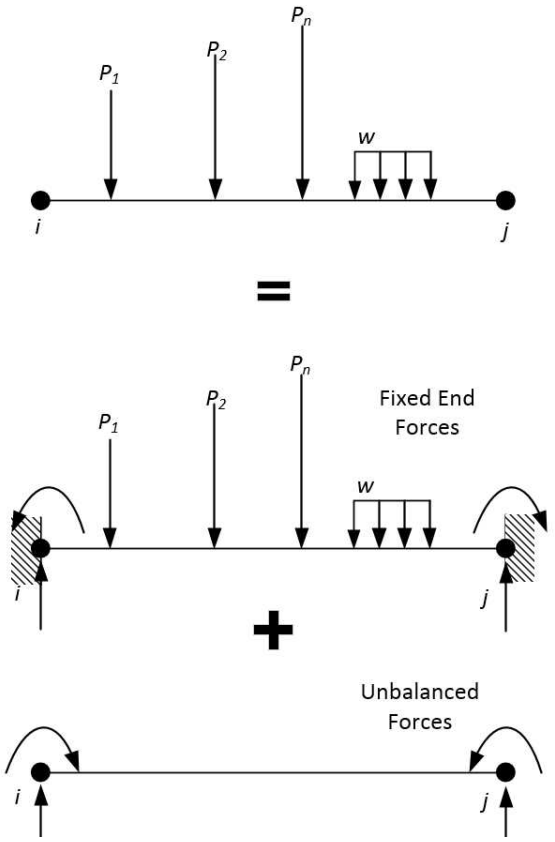

Fig. 11 Load simulation in traditional displacement method.

G. Global Equilibrium Equation

Stiffness matrix for columns and pedestals have been transformed from local axes to the global axes while stiffness matrices for beam, spread footing and soil mass, if any, have already been formulated in term of global axes. After assemblage process, global stiffness matrix for the whole system would be as indicated in equation ((6).

$$[K - K_g]\{d\} = \{0\} \qquad (6)$$

Based on proportional loads indicated in **Fig. 16** and **Fig.** 17 below, axial forces have been determined in the beam and columns then used to generate the geometric stiffness for each element.

H. Solution Techniques

According to reference [10] using the second derivative of elastic curve to approximate its curvature leads to transform the elastic buckling case from a boundary value problem to the eigenvalue problem as indicated in equation ((6).

In its eigen form, the equilibrium equation has a non-trivial solution only when matrix determinate is zero. As only lowest sway and non-sway modes are required, a subspace iterative algorithm has been adopted in this paper to determined eigenvalue and the corresponding eigen vector [11].

III. Model Validation

Proposed finite element model is validated for plane frames with ideal connections indicated in **Fig. 12** and **Fig. 13** below, where the critical loads determined with the proposed model have been compared with

those determined by the traditional analytical approach.

In the traditional approach, the column is firstly isolated from the frame and the restrain due to connection beams is estimated in terms of ratio of column stiffness to beams stiffness presented in equation (**(7**) below.

$$G = \frac{\Sigma I_c / l_c}{\Sigma I_b / l_b} \qquad (7)$$

According to ratio of equation ((**7**), hinge support can be interpreted as a very flexible beam, therefore the ratio approaches to a very high value, a value of 10 is usually adopted, while the fixed support can be interpreted as a very stiff beam and a value of 1.0 is usually adopted [12].

After determination of the ratio ***G***, the effective length factor is computed from the solution of equation (***(8***) indicated below. In the present study, this equation has been solved for different values of G_A and G_B using a Matlab numerical algorithm. The subscripts A and B refer to the joints at the ends of the considered column.

$$\frac{G_A G_B}{4}\left(\frac{\pi}{k}\right)^2 + \left(\frac{G_A + G_B}{2}\right)\left(1 - \frac{\frac{\pi}{k}}{\tan\left(\frac{\pi}{k}\right)}\right) + \frac{2\tan\left(\frac{\pi}{2k}\right)}{\frac{\pi}{k}} - 1 = 0 \qquad (8)$$

Finally, in the traditional method, column critical load is computed from Euler's relation indicated in equation (

(9) below.

$$P_{cr} = \frac{\pi^2 EI}{(kl)^2} \qquad (9)$$

Comparison between the results of the proposed finite element model and the results of the traditional method has been presented in **Fig. 14** and **Fig. 15** below. Good agreement is indicated in these Fig.s, where the difference between the two solution methods can be interpreted in terms of axial deformations that are included in the finite element model while neglected in the traditional method that is based on the traditional slope deflection method, [13].

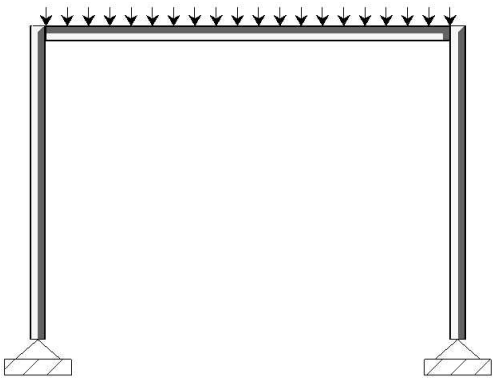

Fig. 12 A plane frame with hinge supports.

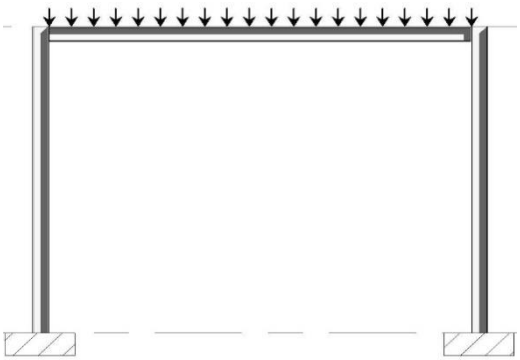

Fig. 13 A plane frame with fixed supports.

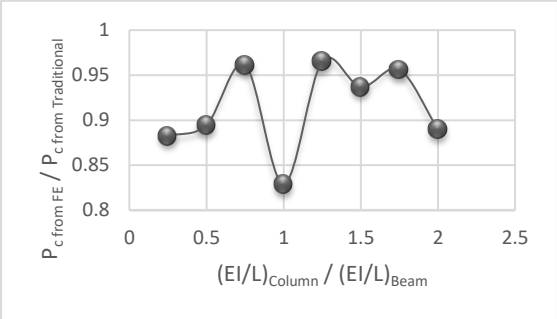

Fig. 14 Validation results for plane frame of Fig. 12.

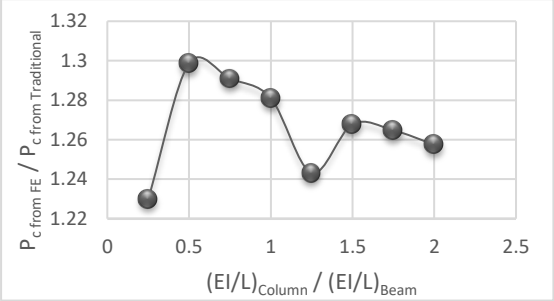

Fig. 15 Validation results for plane frame of Fig. 13.

IV. Case Studies

Different granular soils with SPT value of 10, 20, 30, 40, and 50 have been considered. For each SPT value corresponding soil properties have been determined based on the correlations of section II.E above and presented in **Table. 1** below.

Table. 1 Properties of different granular soils for case studies.

SPT Value	ϕ	$q_{ultimat}$	$k_s, \frac{kPa}{m}$	E_s, kPa	ν_s
10	30.0	301	12040	100000	0.17569
20	32.9	477	19080	200000	0.21826
30	35.6	750	30000	300000	0.25921
40	38.2	1171	46840	400000	0.29854
50	40.8	1828	73120	500000	0.33625

Axial forces for geometric stiffness have been determined in terms proportional loads indicated in **Fig. 16 Fig. 17** below.

Ratios of the critical load computed based on soil mass simulation to those computed based on Winkler model, hinge support, and fixed support for sway and non-sway have been presented in **Table. 2** and **Table. 3**

Respectively. These tables indicate that the more accurate critical loads determined based on soil mass simulation are about four times those determined with hinge support simulation, therefore the hinge support simulation is inaccurate and highly conservative even for flexible soils with SPT of 10. Regarding to fixed support simulation, the tables indicate that it is slightly conservative relative to soil mass simulation.

Relations between critical load computed based on soil mass simulation to the corresponding value determined based on Winkler model are presented in **Fig. 18** and **Fig. 19** for sway and non-sway modes, respectively. Based on a nonlinear regression analysis, the results of the two models for sway mode have been related as indicated in equation ((10) below with a correlation coefficient, R^2, of 0.997, while results of two models for non-sway mode have been related as indicated in equation ((11) with correlation coefficient, R^2, of 0.999.

$$P_{cswaysoilmass} = (-0.039\ln(N) + 1.167)P_{cswayWinkler} \quad (10)$$

$$P_{cnon-swaysoilmass} = (-0.037\ln(N) + 1.153)P_{cnon-swayWinkler} \quad (11)$$

Table. 2 Ratios of critical load determined for soil mass simulation to those loads determined from other simulations for sway mode.

SPT N Value	$\frac{P_{cwithsoilmass}}{P_{cwithWinkler}}$	$\frac{P_{cwithsoilmass}}{P_{cwithHinge}}$	$\frac{P_{cwithsoilmass}}{P_{cwithFixed}}$
10	1.077	0.980	4.41
20	1.049	0.983	4.42
30	1.031	0.984	4.43
40	1.021	0.986	4.43
50	1.015	0.987	4.44

Table. 3 Ratios of critical load determined for soil mass simulation to those loads determined from other simulations for non-sway mode.

SPT N Value	$\frac{P_{cwithsoilmass}}{P_{cwithWinkler}}$	$\frac{P_{cwithsoilmass}}{P_{cwithHinge}}$	$\frac{P_{cwithsoilmass}}{P_{cwithFixed}}$
10	1.077	0.980	4.41
20	1.049	0.983	4.42
30	1.031	0.984	4.43
40	1.021	0.986	4.43
50	1.015	0.987	4.44

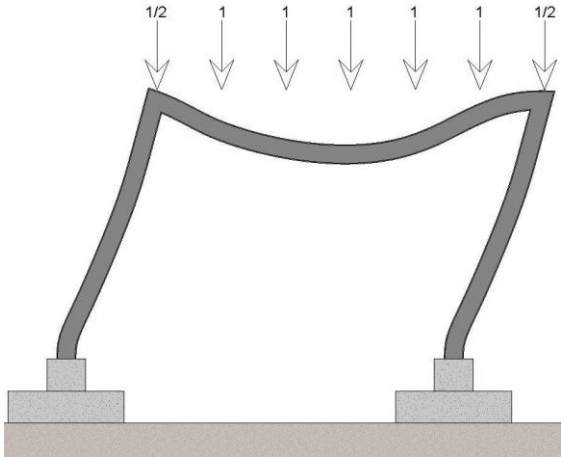

Fig. 16 Sway mode shape and proportional loads that adopted in analysis.

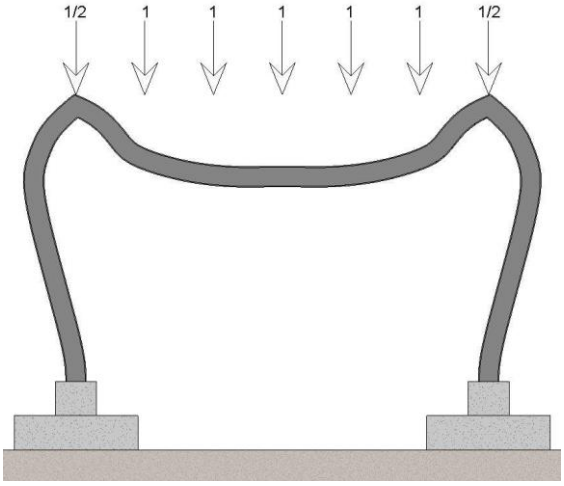

Fig. 17 Non-sway mode shape and proportional loads that adopted in analysis.

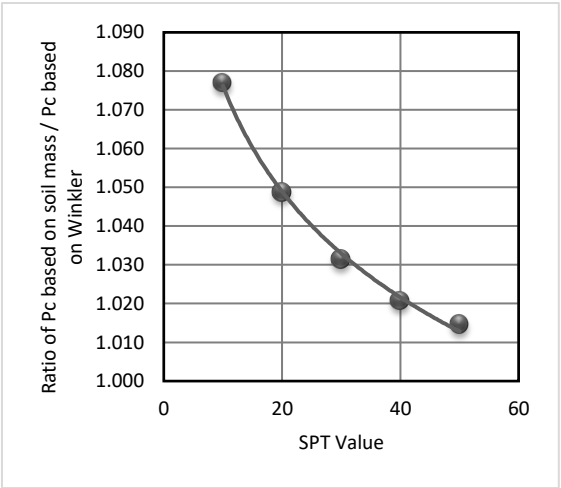

Fig. 18 Ratio of $P_{c\ with\ soil\ mass}$/ $P_{c\ with\ Winkler}$ of sway model for different soil.

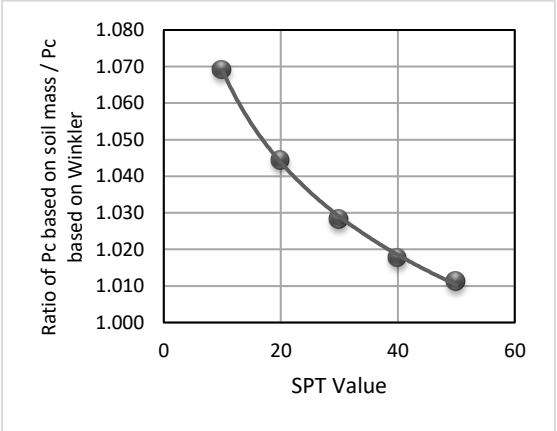

Fig. 19 Ratio of $P_{c\ with\ soil\ mass}$/ $P_{c\ with\ Winkler}$ of non-sway model for different soil.

V. Conclusions

This study shows how different properties and different modeling of dry granular soil can affect buckling loads for sway and non-sway modes of steel portal frames. Two models, namely Winkler model and three-dimensional finite element model, have been adopted to simulate soil behavior in addition to ideal supports of hinge and fixed. All pertained soil properties have been correlated to the SPT values that range from 10 to 50.

From different case studies the following conclusions have been drawn:

1. Critical loads determined based on hinge simulation are so conservative, about 25%, of the more accurate value determined based on soil mass simulation. Therefore, hinge simulation is not recommended even for flexible soils.
2. Although they are slightly conservative, critical loads determined based on fixed support simulation are accurate and can be adopted even for flexible soils.
3. Difference between critical loads computed based on Winkler model and that of soil mass model reach up to 7% for soft soils with SPT value in the range of 10. This conclusion is valid for sway and non-sway buckling modes.
4. Based on regression analyses, logarithmic functions with correlation coefficient, R^2, in the range of 0.99 have been developed to relate critical buckling loads computed from soil mass simulation to those computed from Winkler models.
5. For commercial software that offer only Winkler model to simulate soil, the developed relations are useful to modified critical loads to be more compatible with those determined from soil mass simulation.

VI. Recommendations

For future works, following points are recommended:

1. To consider effects of soil properties and soil simulations on buckling strength of portal frame about minor axes of columns.
2. Other structural systems may be investigated to show how their buckling strengths are affected by soil properties and soil simulation.
3. Cohesive soils with different water level have to be considered to show how their properties and water pore pressure affect buckling loads of frames.

VII. References

[1] S. T. Woolcock, S. Kitipornchai, M. A. Bradfor and G. A. Haddad, Design of Portal Frame Buildings, 4th Edition., Australian Steel Institute, 2011.

[2] S. S. Rao, The Finite Element Method in Engineering, 5th Edition., Elsevier, 2011.

[3] W. McGuire, R. H. Gallagher and R. D. Ziemian, Matrix Structural Analysis, 2nd Edition., Wiley, 2000.

[4] R. D. Cook, Finite Element Modeling for Stress Analysis., John Wiley & Sons, Inc., 1995.

[5] M. E. Harr, Foundations of Theoretical Soil Mechanics., McGraw-Hill Book Company, 1966.

[6] J. E. Bowles, FOUNDATION ANALYSIS AND DESIGN, 5th Edition., McGraw-Hill, 1997.

[7] R. B. Peck, W. E. Hanson and T. H. Thornburn, Foundation Engineering, Second Edition., John Wiley and Sons, Inc., 1974.

[8] B. M. Das, Principles of Foundation Engineering, 7th Edition, CENGAGE Learning, 2011.

[9] R. C. Coates, M. G. Coutie and F. K. Kong, Structural Analysis., London: Nelson, 1972.

[10] S. P. Timoshenko and J. M. Gere, Theory of Elastic Stability. 2nd Edition., Dover Publications, Inc., 1961.

[11] K. J. Bathe, Finite Element Procedures., PHI Learning Private Limited., 1996.

[12] E. H. Gaylord, C. N. Gaylord and J. E. Stallmeyer, Design of Steel Structures, 3rd Edition., McGraw-Hill, 1992.

[13] M. R. Horne and W. Merchant, The Stability of Frames., Pergamon Press, 1965.

تأثير الخصائص والمحاكاة للترب الرملية الجافة على أحمال الانبعاج للهياكل البابية

د.صلاح رحيمة الزيدي
مدرس في قسم الهندسة المدنية
كلية الهندسة / جامعة بغداد
تغريد حسن إبراهيم
مدرس مساعد في قسم الهندسة المدنية
كلية الهندسة / جامعة بغداد
إيهاب غازي
طالب ماجستير في قسم الهندسة المدنية
كلية الهندسة / جامعة بغداد

الخلاصة:-

تهدف هذه الورقة إلى استخدام نماذج مختلفة من العناصر المحددة لإظهار كيفية تأثير ظروف التربة المختلفة ومحاكاتها المختلفة على أحمال الانبعاج للهياكل البابية. كل الترب افترضت حبيبية وجافة، بينما الأساس المنفرد هو الذي افترض لنظام الأساس.

لقد تم اعتماد نوعين من المحاكاة للتربة. في النوع الأول تم نمذجة التربة باستخدام أساس وينكلر وذلك باستبدال وسط التربة المستمر بالنوابض غير المزدوجة ولم يؤخذ بنظر الاعتبار قوى القص بين مواشير التربة المجاورة ولا الصلابة في هذه النمذجة. في النموذج الثاني، تم عزل كتلة التربة تحت الأساس واعتبارها كعنصر طابوقي. في كلا النموذجين تم استخدام رافده وأعمدة لتمثيل نموذج الإطار البابي.

تم تعريف طبيعة التربة الحبيبية من حيث قيمة اختبار الاختراق القياسي، SPT. كل خواص التربة الأخرى بما في ذلك معامل المرونة ونسبة بواسون تم تقديره بالاعتماد على قيمة الاختراق القياسيSPT.

نتائج دراسات الحالة تشير إلى أنه في الأحمال الحرجة لحالة الأساس ذو المسند المفصلي بعيدة عن الأحمال الحرجة المقدرة بصورة أكثر دقة من محاكاة كتلة التربة. من ناحية أخرى، الأحمال الحرجة المقدرة لحالة الأساس ذي المسند الثابت كانت مقاربة للأحمال المقدرة من محاكاة كتلة التربة. هذه الاستنتاجات صالحة حتى للترب الانضغاطية التي لها قيمة SPT بحدود 10.

الأحمال الحرجة المحددة من محاكاة التربة بنموذج وينكلر قريبة من تلك الأحمال التي تم تحديدها من محاكاة كتلة التربة مع فارق لا يزيد عن 7٪ ومع معامل ارتباط قدره 0,99.كما تم اعتماد دالتين لوغاريتميتين لتحليل الانحدار اللاخطي.